Methanol and humidity capacitive sensors based on thin films of MOF nanoparticles

Miguel A. Andrés[†#], Mani Teja Vijjapu[§], Sandeep G. Surya[§], Osama Shekhah[‡], Khaled Nabil Salama[§], Christian Serre[£], Mohamed Eddaoudi[‡], Olivier Roubeau[#], Ignacio Gascón[†#]*

† Departamento de Química Física and Instituto de Nanociencia de Aragón (INA), Universidad de Zaragoza, 50009 Zaragoza (Spain).

Instituto de Ciencia de Materiales de Aragón (ICMA), CSIC and Universidad de Zaragoza, 50009 Zaragoza, Spain.

§ Advanced Membranes & Porous Materials Centre (AMPMC). Computer, Electrical and Mathematical Sciences and Engineering Division, Sensors Lab. King Abdullah University of Science and Technology (KAUST), Thuwal, 23955-6900, Saudi Arabia

‡ Advanced Membranes and Porous Materials Centre (AMPMC). Physical Sciences and Engineering Division, Functional Materials Design, Discovery & Development Lab. King Abdullah University of Science and Technology (KAUST), Thuwal, 23955-6900, Saudi Arabia

£ Institut des Matériaux Poreux de Paris, UMR 8004 CNRS, École Normale Supérieure, École Supérieure de Physique et de Chimie Industrielles de la ville de Paris, PSL University, 75005 Paris, France

KEYWORDS. Metal-organic framework (MOF), MIL-96(Al), nanoparticles (NPs), Langmuir-Blodgett (LB) films, interdigitated electrodes (IDE), capacitive sensor.

ABSTRACT. The successful development of modern gas sensing technologies requires high sensitivity and selectivity coupled to cost-effectiveness, which implies the necessity to miniaturize devices while reducing the amount of sensing material. The appealing alternative of integrating nanoparticles of a porous metal-organic framework (MOF) onto capacitive sensors based on interdigitated electrode (IDE) chips is presented. We report the deposition of MIL-96(Al) MOF thin films via the Langmuir-Blodgett (LB) method on the IDE chips, which allowed the study of their gas/vapor sensing properties. Firstly, sorption studies of several organic vapors like methanol, toluene, chloroform, etc. were conducted on bulk MOF. The sorption data revealed that MIL-96(Al) presents high affinity towards water and methanol. Later on, ordered LB monolayer films of MIL-96(Al) particles of ca. 200 nm were successfully deposited onto IDE chips with homogeneous coverage of the surface in comparison to conventional thin film fabrication techniques such as drop-casting. The sensing tests showed that MOF LB films were selective for water and methanol and short response/recovery times were achieved. Finally, chemical vapor deposition (CVD) of a porous thin film of Parylene C (thickness ca. 250-300 nm) was performed on top of the MOF LB films to fabricate a thin selective layer. The sensing results showed an increase in the water selectivity and sensitivity, while those of methanol showed a huge decrease. These results prove the feasibility of the LB technique for the fabrication of ordered MOF thin films onto IDE chips using very small MOF quantities.

1. INTRODUCTION

Gas/vapor sensors are transducers that generate electrical/optical signals upon adsorbing certain analytes. These sensors are highly demanding, especially for air quality monitoring[1], food processing industries[2] and non-invasive biomedical applications[3]. The key requirements for these applications are sensitivity, selectivity, robustness, low cost, compactness, high response and short recovery time, low power consumption and long lifetime[1, 4]. Recent trends in gas sensing technologies are to address these requirements[4]. With this aim, different transduction mechanisms have been reported using different sensing platforms, such as through the electrical conductivity[4-5], the optical[6] or acoustic[7] responses, chromatography[8] and calorimetry[9]. Among these gas sensing technologies, conductometric-based sensors fulfill many of the required criteria for various applications[10], but selectivity and sensitivity are, generally, low. Moreover these sensors operate at high temperatures resulting in high power consumption[4]. On the other hand, capacitive-based sensors are another attractive class of sensors where capacitance changes due to the change in the dielectric permittivity upon adsorbing the gas/vapor molecule[11]. Capacitive-based sensors are static devices[12] which do not consume high power for sensing, are stable and compact and can be easily integrated with the complementary metal oxide semiconductor (CMOS) based sensing circuits such as capacitance to digital converters (CDCs).[13] These sensors however require additional receptor layers for sensing. Metal-organic frameworks (MOFs) materials are known for selective sorption and high sensitivity for various toxic gases and volatile organic compounds (VOCs)[14], hence the capacitive based MOF sensors[15-20] stand out as better candidates with unique features such as high selectivity, high sensitivity, compactness, long term stability and low power consumption to employ in the gas sensing systems. Another crucial figure of merit of the gas

sensors is that both response and recovery times have to be very short to use them in real time applications[4] which in turn depends on the structure and properties of the receptor layer[20].

Recently, a few reports have shown the interest of gas/vapor sensors based on MOF nanoparticle thin films: Dalstein et al.[21] have developed photonic vapor sensors by dip coating deposition of MIL-101(Cr) colloidal films (nanoparticle size 25 nm) and used a film with thickness of 3.9 μm to study isopropyl alcohol detection at different partial pressures. Zhang et al.[22] have obtained optical sensors with similar response to methanol, ethanol, acetone, n-hexane and cyclohexane. These sensors were based on UiO-66(Zr) crystals (crystal sizes were in the range of 380 - 1057 nm) modified with poly(vinylpyrrolidone) and assembled into a dense monolayer at the air/water interface by a modified Langmuir-Blodgett (LB) technique[23]. Multilayer structures were obtained in this study via the layer-by-layer transfer of monolayers and compared with films fabricated by the solvothermal growth method. Chocarro-Ruiz et al.[24] have reported a CO_2 optical sensor based on ZIF-8(Zn) nanoparticles (optimal size 32 ± 5 nm) spin-coated onto bimodal optical waveguides and the optimal film thickness was found to be 1.15 ± 0.05 μm. Yuan et al.[25] presented a capacitive sensor based on a Mg-MOF-74 grown *in situ* for the selective detection of benzene vapor and carbon dioxide. Its selectivity was further modified toward benzene via post-synthetic functionalization with ethylenediamine.

In this work, we report for the first time the use of MIL-96(Al) MOF LB films as the sensing layer in capacitive based sensors for humidity and methanol sensing (Scheme 1). In a recent contribution[26] we have shown that the LB technique can be used to fabricate thin films of nanoparticles (200 ± 50 nm) of the MOF MIL-96(Al). Additionally, we have proved that a single MOF LB monolayer deposited onto quartz crystal microbalance (QCM) discs can be used upon several CO_2 adsorption/desorption cycles without losing its gas adsorption capacity. Furthermore,

the CO_2 adsorption capacity of these films can be easily increased just via immersing them into water.

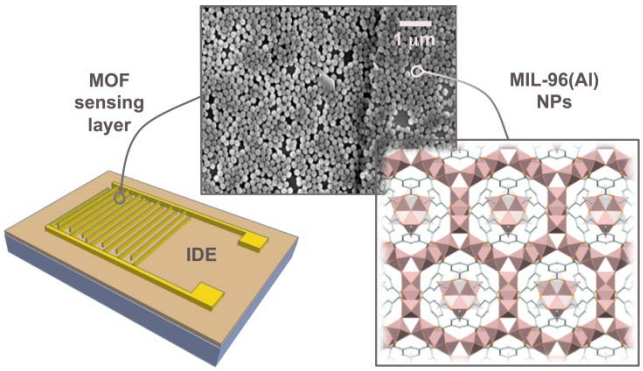

Scheme 1. Illustration of the structure of the used IDEs showing MOF LB film characterization by SEM. A schematic representation of MIL-96(Al) structure is also included.

In this context, the LB technique provides some relevant advantages for the development of MOF nanoparticle thin films. The MOF amount used in film preparation is very small, the total film thickness can be controlled, since a single monolayer is deposited in each transfer, and several kinds of substrates can be used for film deposition. Moreover, in the case of MIL-96(Al), it was not necessary to add any surfactant to obtain dense monolayers at the air-water.[26] Additionally, MIL-96(Al) is very interesting for the development of MOF based sensors because it possesses narrow pores and contains three different types of cavities, which can provide selectivity to different analytes. Besides, it is a water stable MOF that presents also remarkable hydrothermal and thermal stability.

In this study, we have deposited MIL-96(Al) LB films onto Si/SiO_2 substrates incorporating gold interdigitated electrodes (IDEs) and explored their use as gas/vapor sensing layer for capacitive-based sensors for water or methanol sensing. LB films showed better coverage, shorter

response and recovery times and faster response than drop-cast thin films, which demonstrate the advantages of the use of MOF LB films for the development of gas/vapor sensing devices. We were also able to improve the sensitivity and selectivity of MIL-96(Al) LB films for water via the chemical vapor deposition (CVD) of a porous thin film of Parylene C on top of the LB MOF thin films.

2.- MATERIALS AND METHODS

Sorption isotherms on bulk MOF were obtained using the volumetric method with a VStar (Quantachrome) sorption analyser operated at 25 ºC. A sample amount of ca. 20 mg was used for each measurement. MIL-96(Al) was activated at 100 ºC under vacuum (10^{-3} mbar) for 16 h prior to each sorption experiment.

Suspension and film optimization have been already reported by some of us[26]. Briefly, suspensions of MIL-96(Al) particles were prepared using chloroform (Macron, >99.8%) and an ultrasonication probe-type device (Hielscher UP400S ultrasonic processor, H3 type tip) operated continuously at 50% amplitude during 30 minutes. Langmuir-Blodgett films were fabricated onto IDEs at a surface pressure of 30 mN/m by vertical dipping at 1 mm/min. Langmuir-Schaefer samples were fabricated by holding the substrates parallel to the surface using a horizontal dipping clamp with a suction cap of 7 mm diameter (KSV KN-006). IDEs were lowered at a vertical speed of 1 mm/min until the substrate touched the water surface. Then, they were raised at a rate of 10 mm/min of vertical speed.

Si wafers [100] of 100 Ω/cm resistivity with 2 µm thermally grown SiO_2 were purchased from Si-Mat (Germany). The fabrication of interdigitated structures for electrodes (IDEs) was done at the KAUST Nanofab and the fabrication flow is as follows: firstly Si/SiO_2 wafers were cleaned

ultrasonically in acetone, isopropyl alcohol, and DI water for 10 minutes each and dried on top of a hot plate at 120 °C for 15 minutes to get rid of moisture. Subsequently, we adopted lithography process as reported by some of us[20] to form the IDE patterns and lift-off technique is used after physical vapor deposition of metals using DC magnetron sputtering to generate the IDEs with a gap of 30 µm between the fingers. DC sputtering was performed at 400W in presence of Ar plasma to obtain thicknesses of 10 nm of titanium (Ti) and 200 nm of gold (Au) which serves as interdigitated electrodes. A scheme of the fabricated device is shown in Figure S1. After the successful deposition of MOF using the Langmuir-Blodgett technique, vapor and gas sensing tests were performed on a custom gas setup[20]. Capacitance-time measurements were carried out using a Keysight E4980A LCR meter at 100kHz. A Labview-based interface was used to acquire data from LCR meter and to control mass flow controllers (MFCs). Two gas currents were used, one was flown into the bubbler containing the liquid (wet current) and the other one was used as dilution (dry current). VOC source was immersed in a F12-MA Julabo thermostatic bath for precise control of the vapor pressure. All the gas/vapor testing of LB capacitive sensors were done at a fixed flow rate of 200 sccm (standard cubic centimeters per minute) using nitrogen as carrier gas. Total gas flow was monitored with a mass flow meter (MFM) before entering the measurement cell and it is based on the following equation: $F_{total}=(1+\alpha)F_{wet} + F_{dry}$, where F_{wet} and F_{dry} are the carrier flow rates in the wet and dry current respectively and α is the ratio of the saturated vapor pressure at chiller temperature to the pressure of carrier gas entering the bubbler. Vapor concentration was calculated as parts per million (ppm) in volume according to the equation: $C_{ppm}=10^6(\alpha F_{wet}/F_{total})$.

For the deposition of Parylene C on top of LB films a protocol similar to one previously described by some of us was used[27]. Briefly, Parylene C dimer crystals (500 mg) were heated at

175 °C in a precursor chamber under vacuum to generate dimeric vapors. These vapors were passed through another chamber at 650 °C to cleave them to monomer gas molecules. Then, monomer gas was let into a third chamber where the IDE devices were kept under vacuum (10^{-6} mbar) at room temperature, and Parylene C gets deposited and self-assembled to form the polymer thin film) on top of Si/SiO_2/MOF LB substrate.

SEM images were obtained using a Zeiss Merlin field emission scanning electron microscope (FESEM) equipped with a Gemini II column and operated at 5 KV with a beam current of 120 pA. All samples were coated with a layer of 5 nm of Iridium. Optical microscopy images were taken using a Zeiss AX10 optical microscope. Grazing incidence X-ray diffraction (GIXRD) characterization of LB films deposited onto IDEs was done on an Empyrean diffractometer (PANalytical) equipped with a Pixcell 1D medpix3 detector. Measurements were conducted using 45 kV of generator voltage and 40 mA of tube current. Scans were obtained in the open detector mode using a grazing incidence angle of 0.16º.

3.- RESULTS AND DISCUSSION

3.1.- Sorption isotherms of MIL-96(Al) NPs

MIL-96(Al) is known to show high affinity to water as previously reported by Serre et al.[28] In order to explore the use of MIL-96(Al) for vapor sensing applications, we focused on the use of 200 nm nanoparticles (NPs) of the same MOF, which are appropriate for Langmuir-Blodgett thin film fabrication[26] and we studied the adsorption properties of these MOF NPs for water and other different organic vapors (Figure 1). High affinity for water was maintained in the nanoparticles together with a good affinity for methanol. The water sorption isotherm is slightly different from the one previously reported[28], probably because of the smaller size of the particles and different

shape. Acetone and ethanol showed moderate affinities although lower uptakes were reached in comparison to water and methanol, probably because of the difference in kinetic diameters (4.5 and 4.6 Å for ethanol and acetone, 3.6 and 2.6 Å for methanol and water). Finally, for chloroform and toluene the low initial uptake and the continuous rise with increasing relative pressure is representative of low affinity. Also, kinetics for each equilibrium point in these two solvents were much longer in comparison to water and methanol. These results showed that this material could be a good candidate for selective sensing of water and methanol vapors.

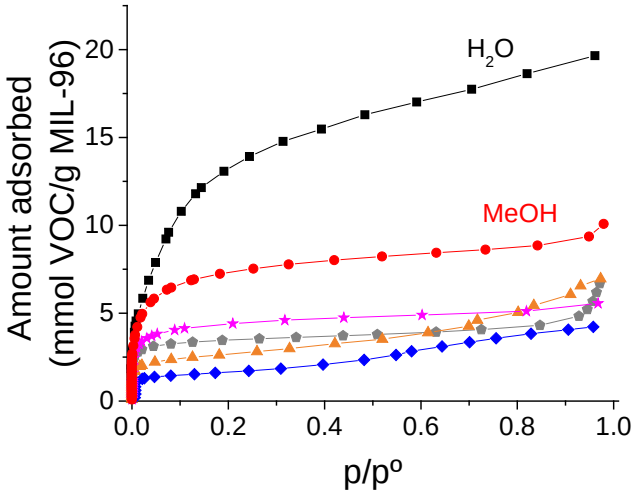

Figure 1. Sorption isotherms for MIL-96(Al) NPs of 200 nm of water (black ■), methanol (red ●), ethanol (pink ★), acetone (grey ⬟), chloroform (orange ▲) and toluene (blue ◆) vapors. Only sorption branches are shown for clarity purposes.

3.2.- Langmuir-Blodgett film deposition on IDEs and characterization

Inspired by our previous work[26], LB films of MIL-96(Al) NPs of 200 nm were successfully deposited onto Si/SiO_2 substrates incorporating IDEs (see Figure S1 for a schematic representation). LB films of 1 and 2 layers were prepared and characterized using scanning electron microscopy (SEM) (Figure 2). SEM images showed good quality films deposited both on

top of gold electrodes and in-between the fingers, despite the non-homogeneity of the surface of the substrate. This fact proves that the layer is rigid enough not to break, and at the same time sufficiently flexible to allow a homogeneous coverage of patterned surfaces. A second cycle of LB deposition results in only a partial second layer deposition of MOF NPs, which more likely is a consequence of inter-particle spacing. These results, though, clearly demonstrate the ability of the LB technique to provide an efficient homogeneous coating of MOF with homogeneous particle size and minimal material amounts. Since this is essential for the correct functioning of IDEs, LB appears as a powerful method to fabricate MOFs as thin films and their application as sensors.

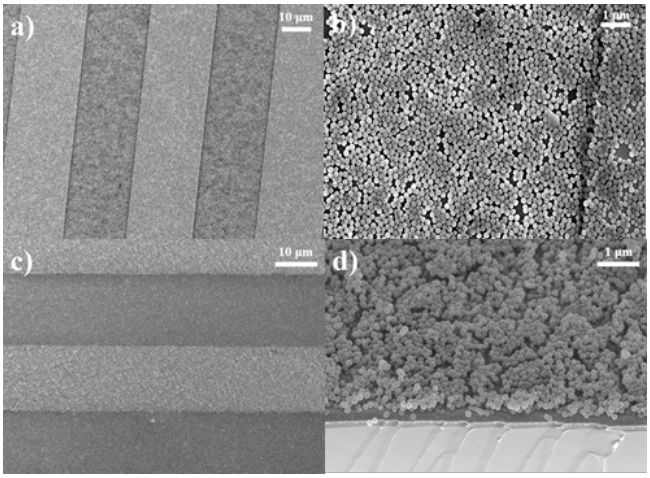

Figure 2. SEM images of MIL-96(Al) LB films deposited onto IDE chips: 1 layer (a, b) and 2 layers (c, d). (a), (b) and (c) images correspond to top-view; (d) image of the 2-layered sample was obtained at 45º tilt angle. Scale bars correspond to 1 µm (a, c) and 10 µm (b, d).

The use of horizontal deposition (Langmuir-Schaefer) was also explored but as shown in Figure S1, some cracks are observed in the LS sample and the films obtained are less homogeneous than LB films, probably because of the non-regular surface of the substrates and the relative rigidity of

the Langmuir film. Hence, vertical deposition is the optimal method for the fabrication of the sensing layer in these patterned substrates.

Drop-cast samples using suspensions in chloroform were also prepared for the sake of comparison. However, the sensor coverage was poor using this method, with the formation of agglomerates which resulted in the spaces between the fingers being not fully covered (Figure S2).

In order to check that the cristallinity of the MOF is preserved upon film deposition, GIXRD was performed on LB coated IDE substrates. As shown in Figure 3, the crystalline structure of the MOF remains unaltered. The characteristic peak of gold at 38.2º can also be seen although signal is low due to the low detection angle used.

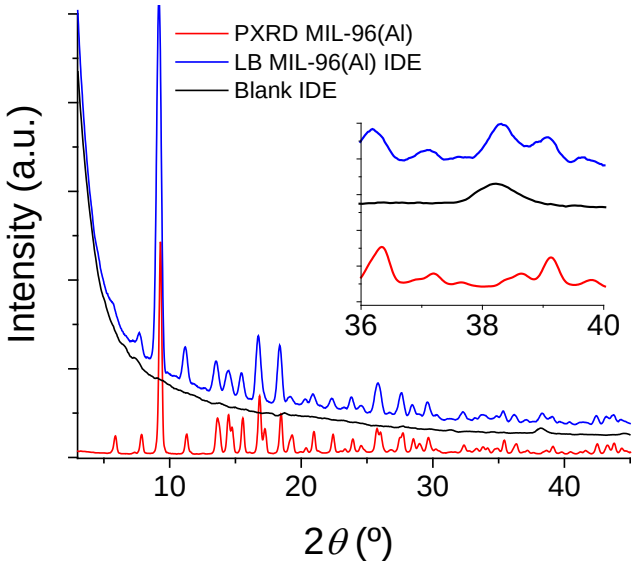

Figure 3. GIXRD diffractogram of IDE + LB MIL-96(Al) (blue —). Inset: detail on 36-40º to show the Au peak. For comparison purposes, PXRD of the MOF (red —) and GIXRD of a blank IDE (black —) are also included.

3.3 Vapor and gas sensing properties

MOF activation is critical for sensing application since the final purpose is obtaining a thin MOF film free of guest molecules. The sensors fabricated required a previous activation step overnight at 100 ºC in a vacuum oven, especially to remove water molecules due to the high affinity of MIL-96(Al) to water. To investigate the sensing properties of the films, response to water and different volatile organic compounds vapors was measured at different concentrations from 0 to 5000 ppm. Figure 4 shows the normalized response of the MIL-96(Al) LB based IDEs, where C is the baseline capacitance of the device (stable reading while flowing pure N_2) and ΔC is the change in the capacitance between the value at a given concentration and the baseline (i.e. $\Delta C=C_2-C_1$, C_2 is the capacitance at the desired concentration and C_1 the baseline capacitance with pure N_2).

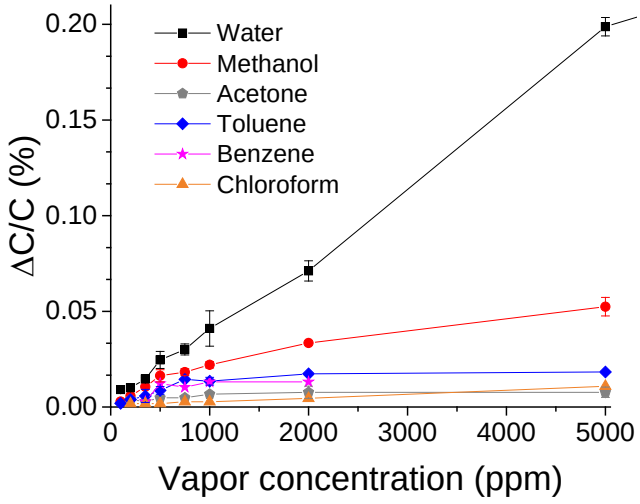

Figure 4. Selectivity study of LB-based MIL-96(Al) IDEs for different vapors: water (black ■), methanol (red ●), acetone (grey ⬟), toluene (blue ◆), benzene (pink ★), chloroform (orange ▲). Sensitivity values are expressed as $\Delta C/C$ (%). Error bars correspond to standard deviation from the measurement of at least two different samples. Error bars in some points are not visible because of the size of the symbols.

The IDEs showed high affinity for water and methanol vapor, whereas the sensitivity for acetone, toluene, chloroform and benzene vapors was much lower. In addition, different relevant gases were also tested (namely CH_4, CO_2, SO_2, H_2, NH_3), where all of them showing responses comparable to those of toluene, benzene and chloroform (Figure S3). Then, it can be deduced that these sensors were selective to water and methanol.

Response and recovery time for water and methanol were within 10-15 minutes for each step both for LB 1 and 2 layers. Moreover, response of LB 2-layered samples is in average 1.5 times higher than the response of 1-layered samples (Figure S4), in accordance to the SEM images, which showed an average of 1.5 deposited layers.

3.4 Water and methanol sensing properties

One of the key aspects of gas sensors is their selectivity and, as it has been previously shown, response to water is similar to that of methanol until 500 ppm, increasing at higher concentration values. To further characterize water/methanol selectivity of the sensors, higher concentration values were studied for these two vapors (Figure 5b). It can be seen that from 5000 ppm the response for water is around 4 times that of methanol. More interestingly, chips can be regenerated along all the concentration range studied as it can be seen in the capacitive curve response for water (Figure 5a).

Linearity of the response to water was also analyzed (Figure S5), where the IDEs show linear response until 20% relative humidity (RH), with a sensitivity of 0.0088 ($100 \cdot \Delta C/C$) per percent of RH and a limit of detection of 0.21 % RH.

One interesting feature of sensors is their recyclability for several sensing experiments. IDEs proved to be reliable for recycling experiments at 50 and 90 % RH (Figure 6). Stability was not

studied in depth but IDEs response for three different experiments in a week was compared and devices proved to be stable (Figure S6).

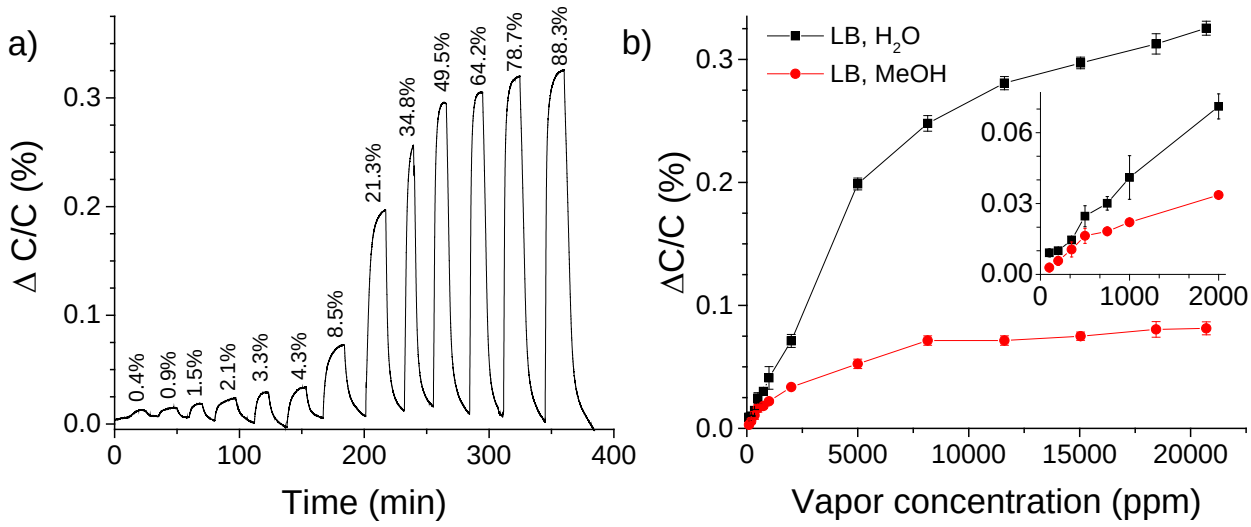

Figure 5. a) Capacitive response curve for water vapor for MIL-96(Al) LB IDEs. Values above the peaks represent the corresponding relative humidity measured at 20 ºC. b) Normalized capacitive response of IDEs to water (black ■) and methanol (red ●). Inset: Response of IDEs in the low ppm range. Error bars correspond to standard deviation from the measurement of at least two different samples. Error bars in some points are not visible because of the size of the symbols.

The response of the LB-based devices has been compared with commercially available sensors for water and methanol in Table S1 of the supporting information. As can be observed the performance of the MOF-based capacitive sensor could be competitive, especially for methanol sensing while the water response could be still improved. Finally, methanol response of IDEs fabricated with conventional drop-casting of the MOF particles has also been compared with the LB-based sensors. Drop-cast devices showed higher normalized responses but with much higher response and recovery times than those of LB devices, being increased from 10-15 minutes of LB devices to 50 minutes of drop-cast samples (Figure S7). LB films led to better coverage and more

homogeneous films in comparison to drop-cast films, as evidenced by SEM (see Figure 2 for LB and Figure S2 for drop-cast SEM images), hence accounting for the better response and recovery observed on the sensors.

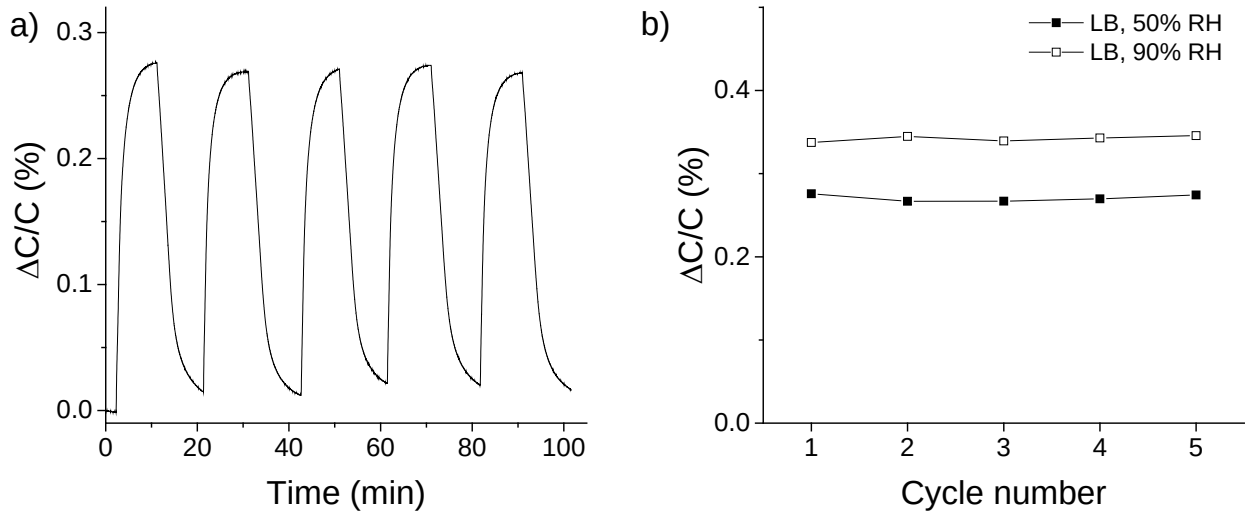

Figure 6. a) Capacitive response curve for recycling experiments performed on MIL-96(Al) LB IDEs at 50 % RH. b) Normalized capacitive response for water vapor recycling experiments on MIL-96(Al) LB IDEs at 50 % (■) and 90 % RH (□). Relative humidity was measured at 20 ºC.

3.5 Improvement of water/methanol selectivity

In order to further improve the selectivity to either water or methanol, an additional selective layer was deposited on top of the LB film. The idea of this selective layer is to act as a barrier to either prevent/decrease water or methanol diffusion, without changing significantly the response to the other analyte. Parylene C has been widely used in the last decades as a protective and insulating layer on medical and electronic devices[29-30]. However, some studies have shown that thin films (below 1 μm) of polymer Parylene C deposited onto non-conventional surfaces (e.g. on top of liquids) show porosity. As reported by Binh-Khiem and coworkers[31], this porosity comes from the interaction of the Parylene monomers with the liquid surface, which modifies the

polymerization process. They showed cross-sectional SEM images revealing that the surface exposed to the air is similar to conventional Parylene C (dense and smooth) in contrast to the lower surface, which is in contact with the liquid, which appeared as a porous network of polymer islands.

In our study, a thin Parylene C film was deposited on top of the MIL-96(Al) LB layer by CVD. The resulting polymer film has a thickness of approximately 250-300 nm as revealed by cross-sectional SEM images (Figure 7). MOF particles are sandwiched between the IDE surface and the Parylene C film. Interestingly, the same effect described by Binn-Khiem et al.[31] is observed in our case, and Parylene C film appears to show a porous texture on the side exposed to the MOF NPs.

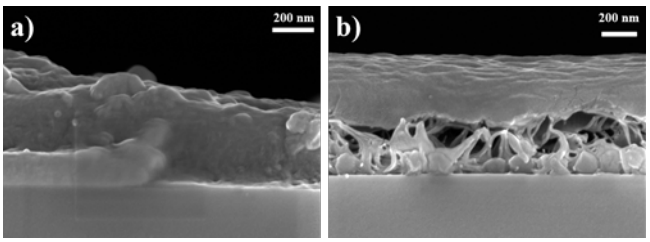

Figure 7. SEM cross-sectional images (90º) of pure Parylene C film (a) and LB MIL-96(Al) + Parylene C film (b) deposited onto IDEs. Scale bar corresponds to 200 nm.

In order to study the effect of the polymer film on the sensitivity, we studied the response of these MOF LB + Parylene C devices for water and methanol vapors. Four different concentrations were measured in the range from 0 to 8500 ppm. Interestingly, the effect observed was a huge increase in water selectivity and response, with a drastic decrease in methanol sensitivity (Figure 8). Moreover, response and recovery times only increased by approximately 5 minutes (Figure S8). Similar studies were performed on IDEs bearing only the polymer film deposited by CVD,

however, the response was negligible. Our hypothesis is that on the one hand the polymer is acting as a porous network with a sieving effect based on the size of water and methanol molecules (kinetic diameters are respectively ~2.6 and ~3.6 Å). On the other hand, the polymer probably also helps water to pre-concentrate on/near the MOF particles acting as a kind of barrier, hence the almost 1.5 times higher response observed in comparison to the untreated LB samples. This approach opens up a promising way to increase selectivity on LB-based sensors.

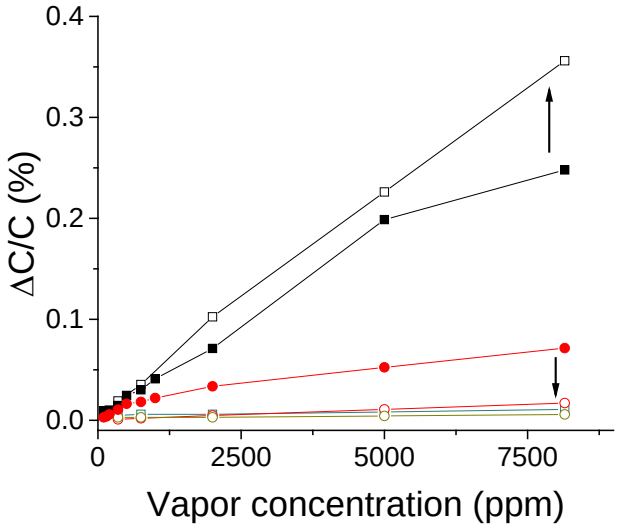

Figure 8. Normalized responses, ΔC/C (%), of IDE devices to water and methanol: MOF LB + Parylene C film (black □ water, red ○ methanol), Parylene C film (blue □ water, green ○ methanol) and untreated MOF LB (black ■ water, red ● methanol). Arrows indicate the effect of Parylene C film additional layer on LB samples.

3.6.- Methanol and humidity sensing

The improvement of selectivity to water by Parylene C deposition on top of LB films provides an opportunity to sense both methanol and humidity by implementing two LB capacitive sensors in a single system sensor array. The proposed schematic logic system is shown in Figure 9 where we assume that MIL-96(Al) LB + Parylene C layer IDE (referred to as C1) and MIL-96(Al) LB

IDE (referred to as C2) are connected together to a capacitance to digital converter (CDC) which is feeding the resultant of these capacitances (C_{eff}). As discussed in the previous section, the response of C1 is high only for humidity while C2 has high response for humidity and moderate response for methanol. Therefore, this configuration will result in very high capacitive response (C_{eff}= C1+C2) for humidity and moderate response for methanol (C_{eff}=C2) (see table in Figure 9).

By defining the thresholds in the system, it would be feasible to detect both humidity and methanol.

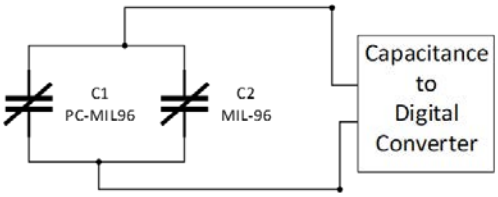

Ambient Condition	Variation in ΔC1 (MIL-96(Al) LB + Parylene C layer IDE)	Variation in ΔC2 (MIL-96(Al) LB IDE)	C_{eff} Input to the CDC
Water	High	High	ΔC1+ ΔC2 (Very High)
Methanol	Low (Almost Zero)	Moderate	ΔC2 (Moderate)

Figure 9. Diagram and truth table of the logic system proposed for methanol and humidity sensing using our LB-based sensors.

4.- CONCLUSIONS

In this work, we have demonstrated that it is possible to deposit thin films of MIL-96(Al) NPs onto Si/SiO_2 substrates incorporating IDEs, without any substrate functionalization thanks to the Langmuir-Blodgett technique. Interestingly, the thickness of the receptor layer corresponds to just one monolayer of particles (ca. 200 nm), that maintain crystallinity upon film transference. The sensors obtained are highly and moderately selective to water and methanol, respectively, compared with the response obtained for other volatile compounds and relevant gases. Response

and recovery times are faster using a single MOF monolayer (about 10-15 minutes) than drop-cast films (about 50 minutes). Furthermore, LB-based sensors are regenerable to several sensing cycles and stable with time for at least one week. Eventually, a protective thin Parylene C polymeric film on top of the MOF film allows increasing significantly the sensor selectivity to water, while decreasing the response to methanol, probably resulting from a sieving effect. Altogether, our results pave the way to implementing arrays of LB-based IDE sensors for simultaneous detection of water and methanol using a logic-based system.

ASSOCIATED CONTENT

Supporting Information

Figures showing additional details about Langmuir-Blodgett film formation onto IDEs and capacitive responses of these devices on additional experiments can be found in the supporting information. This material is available free of charge via the Internet at http://pubs.acs.org.

AUTHOR INFORMATION

Corresponding Author

*Ignacio Gascon. E-mail: igascon@unizar.es

Author Contributions

The manuscript was written through contributions of all authors. All authors have given approval to the final version of the manuscript.

Funding Sources

Spanish MINECO and FEDER (projects MAT2016-78257-R and MAT2017-86826-R). Aragon Government (DGA) and the ESF (research group E31_17R). Spanish Government FPU grant (Formación de Profesorado Universitario, FPU14/05367) and a short term mobility FPU grant (EST18/00291). Visiting Student Program (King Abdullah University of Science and Technology and Advanced Membranes and Porous Materials Center).

ACKNOWLEDGMENT

The research leading to these results has received funding from Spanish MINECO and FEDER (projects MAT2016-78257-R and MAT2017-86826-R), the Aragon Government (DGA) and the ESF (research group E31_17R). Miguel A. Andrés acknowledges the support of Ministerio de Educación from the Spanish Government under a FPU grant (Formación de Profesorado Universitario, FPU14/05367) and a short term mobility FPU grant (EST18/00291) and of King Abdullah University of Science and Technology and Advanced Membranes and Porous Materials Center under the Visiting Student Program.

The authors acknowledge the use of the Laboratorio de Microscopías Avanzadas (LMA) at the Instituto de Nanociencia de Aragón (INA, Universidad de Zaragoza).

The authors also thank Dr. Prashant Batt and Dr. Zied Ouled for technical support in gas sorption experiments and Dr. Guillermo Antorrena for technical support in GIXRD experiments.

ABBREVIATIONS

CDC, capacitance to digital converter; CMOS, complementary metal oxide semiconductor; CVD, chemical vapor deposition; FESEM, field emission scanning electron microscope; GIXRD, grazing incidence X-ray diffraction; IDE, interdigitated electrodes; LB, Langmuir-Blodgett; LS,

Langmuir-Schaefer; MOF, metal-organic framework; NPs, nanoparticles; PXRD, powder X-ray diffraction; RH, relative humidity; VOC, volatile organic compound.

REFERENCES

1. Cavaliere, A.; Carotenuto, F.; Di Gennaro, F.; Gioli, B.; Gualtieri, G.; Martelli, F.; Matese, A.; Toscano, P.; Vagnoli, C.; Zaldei, A. Development of Low-Cost Air Quality Stations for Next Generation Monitoring Networks: Calibration and Validation of PM2.5 and PM10 Sensors. Sensors (Basel) 2018, 18 (9), 2843.

2. Gliszczyńska-Świgło, A.; Chmielewski, J. Electronic Nose as a Tool for Monitoring the Authenticity of Food. A Review. Food Anal. Methods 2016, 10 (6), 1800-1816.

3. Jia, Z.; Patra, A.; Kutty, V. K.; Venkatesan, T. Critical Review of Volatile Organic Compound Analysis in Breath and In Vitro Cell Culture for Detection of Lung Cancer. Metabolites 2019, 9 (3).

4. Liu, X.; Cheng, S.; Liu, H.; Hu, S.; Zhang, D.; Ning, H. A Survey on Gas Sensing Technology. Sensors (Basel) 2012, 12 (7), 9635-9665.

5. Wang, C.; Yin, L.; Zhang, L.; Xiang, D.; Gao, R. Metal Oxide Gas Sensors: Sensitivity and Influencing Factors. Sensors 2010, 10 (3), 2088-2106.

6. Bogue, R. Detecting Gases With Light: a Review of Optical Gas Sensor Technologies. Sens. Rev. 2015, 35 (2), 133-140.

7. Petculescu, A.; Hall, B.; Fraenzle, R.; Phillips, S.; Lueptow, R. M. A Prototype Acoustic Gas Sensor Based on Attenuation. J. Acoust. Soc. Am. 2006, 120 (4), 1779-1782.

8. Kim, K.-H. Performance Characterization of the GC/PFPD for H_2S, CH_3SH, DMS, and DMDS in Air. Atmos. Environ. 2005, 39 (12), 2235-2242.

9. Ng, K. T.; Boussaid, F.; Bermak, A. A CMOS Single-Chip Gas Recognition Circuit for Metal Oxide Gas Sensor Arrays. IEEE T Circuits-I: Regular Papers 2011, 58 (7), 1569-1580.

10. Wang, C.; Yin, L.; Zhang, L.; Xiang, D.; Gao, R. Metal Oxide Gas Sensors: Sensitivity and Influencing Factors. Sensors (Basel) 2010, 10 (3), 2088-2106.

11. Sapsanis, C.; Omran, H.; Chernikova, V.; Shekhah, O.; Belmabkhout, Y.; Buttner, U.; Eddaoudi, M.; Salama, K. N. Insights on Capacitive Interdigitated Electrodes Coated with MOF Thin Films: Humidity and VOCs Sensing as a Case Study. Sensors (Basel) 2015, 15 (8), 18153-18166.

12. Omran, H.; Salama, K. N. in Design and Fabrication of Capacitive Interdigitated Electrodes for Smart Gas Sensors, 2015 IEEE 3rd International Conference on Smart Instrumentation, Measurement and Applications (ICSIMA), 24-25 Nov. 2015; 2015; pp 1-4.

13. Omran, H.; Arsalan, M.; Salama, K. N. 7.9 pJ/Step Energy-Efficient Multi-Slope 13-bit Capacitance-to-Digital Converter. IEEE T Circuits-II: Express Briefs 2014, 61 (8), 589-593.

14. Fang, X.; Zong, B.; Mao, S. Metal-Organic Framework-Based Sensors for Environmental Contaminant Sensing. Nano-micro Lett 2018, 10 (4), 64.

15. Chappanda, K. N.; Tchalala, M. R.; Shekhah, O.; Surya, S. G.; Eddaoudi, M.; Salama, K. N. A Comparative Study of Interdigitated Electrode and Quartz Crystal Microbalance Transduction Techniques for Metal(-)Organic Framework-Based Acetone Sensors. Sensors (Basel) 2018, 18 (11).

16. Tchalala, M. R.; Belmabkhout, Y.; Adil, K.; Chappanda, K. N.; Cadiau, A.; Bhatt, P. M.; Salama, K. N.; Eddaoudi, M. Concurrent Sensing of CO_2 and H_2O from Air Using Ultramicroporous Fluorinated Metal-Organic Frameworks: Effect of Transduction Mechanism on the Sensing Performance. ACS Appl. Mater. Interfaces 2019, 11 (1), 1706-1712.

17. Yassine, O.; Shekhah, O.; Assen, A. H.; Belmabkhout, Y.; Salama, K. N.; Eddaoudi, M. H_2S Sensors: Fumarate-Based fcu-MOF Thin Film Grown on a Capacitive Interdigitated Electrode. Angew. Chem. Int. Ed. Eng. 2016, 55 (51), 15879-15883.

18. Chernikova, V.; Yassine, O.; Shekhah, O.; Eddaoudi, M.; Salama, Khaled N. Highly Sensitive and Selective SO_2 MOF Sensor: the Integration of MFM-300 MOF as a Sensitive Layer on a Capacitive Interdigitated Electrode. J. Mater. Chem. A 2018, 6 (14), 5550-5554.

19. Assen, A. H.; Yassine, O.; Shekhah, O.; Eddaoudi, M.; Salama, K. N. MOFs for the Sensitive Detection of Ammonia: Deployment of fcu-MOF Thin Films as Effective Chemical Capacitive Sensors. ACS Sens. 2017, 2 (9), 1294-1301.

20. Chappanda, K. N.; Chaix, A.; Surya, S. G.; Moosa, B. A.; Khashab, N. M.; Salama, K. N. Trianglamine Hydrochloride Crystals for a Highly Sensitive and Selective Humidity Sensor. Sens. Actuator B-Chem. 2019, 294, 40-47.

21. Dalstein, O.; Gkaniatsou, E.; Sicard, C.; Sel, O.; Perrot, H.; Serre, C.; Boissière, C.; Faustini, M. Evaporation-Directed Crack-Patterning of Metal–Organic Framework Colloidal Films and Their Application as Photonic Sensors. Angew. Chem. Int. Ed. Eng. 2017, 56 (45), 14011-14015.

22. Zhang, R.; Zhang, D.; Yao, Y.; Zhang, Q.; Xu, Y.; Wu, Y.; Yu, H.; Lu, G. Metal–Organic Framework Crystal-Assembled Optical Sensors for Chemical Vapors: Effects of Crystal Sizes and Missing-Linker Defects on Sensing Performances. ACS Appl. Mater. Interfaces 2019, 11 (23), 21010-21017.

23. Lu, G.; Cui, C.; Zhang, W.; Liu, Y.; Huo, F. Synthesis and Self-Assembly of Monodispersed Metal-Organic Framework Microcrystals. Chem. Asian J. 2013, 8 (1), 69-72.

24. Chocarro-Ruiz, B.; Pérez-Carvajal, J.; Avci, C.; Calvo-Lozano, O.; Alonso, M. I.; Maspoch, D.; Lechuga, L. M. A CO_2 Optical Sensor Based on Self-Assembled Metal–Organic Framework Nanoparticles. J. Mater. Chem. A 2018, 6 (27), 13171-13177.

25. Yuan, H.; Tao, J.; Li, N.; Karmakar, A.; Tang, C.; Cai, H.; Pennycook, S. J.; Singh, N.; Zhao, D. On-Chip Tailorability of Capacitive Gas Sensors Integrated with Metal–Organic Framework Films. Angew. Chem. Int. Ed. Eng. 2019, 58 (40), 14089-14094.

26. Andrés, M. A.; Benzaqui, M.; Serre, C.; Steunou, N.; Gascón, I. Fabrication of Ultrathin MIL-96(Al) Films and Study of CO_2 Adsorption/Desorption Processes Using Quartz Crystal Microbalance. J. Colloid Interface Sci. 2018, 519, 88-96.

27. Surya, S. G.; Samji, S. K.; Dhamini, P.; Ganne, B. P.; Sonar, P.; Rao, V. R. A Spectroscopy and Microscopy Study of Parylene-C OFETs for Explosive Sensing. IEEE Sens. J. 2018, 18 (4), 1364-1372.

28. Benoit, V.; Chanut, N.; Pillai, R. S.; Benzaqui, M.; Beurroies, I.; Devautour-Vinot, S.; Serre, C.; Steunou, N.; Maurin, G.; Llewellyn, P. L. A Promising Metal–Organic Framework

(MOF), MIL-96(Al), for CO_2 Separation under Humid Conditions. J. Mater. Chem. A 2018, 6 (5), 2081-2090.

29. Marszalek, T.; Gazicki-Lipman, M.; Ulanski, J. Parylene C As a Versatile Dielectric Material for Organic Field-Effect Transistors. Beilstein J. Nanotechnol. 2017, 8, 1532-1545.

30. Tan, C. P.; Craighead, H. G. Surface Engineering and Patterning Using Parylene for Biological Applications. Materials 2010, 3 (3), 1803-1832.

31. Binh-Khiem, N.; Matsumoto, K.; Shimoyama, I. Tensile Film Stress of Parylene Deposited on Liquid. Langmuir 2010, 26 (24), 18771-18775.

SYNOPSIS